


Equation of state and correlation functions of hypernuclear matter within the lowest order constrained variational method

M. Shahrabaf, H. R. Moshfegh , and M. Modarres

Department of Physics, University of Tehran, P.O. Box 14395-547, Tehran, Iran



(Received 28 May 2019; published 21 October 2019)

The lowest order constrained variational method is reformulated to find the equation of state of hypernuclear matter. For the nucleon-nucleon interaction we employed the well-known Argonne V18 (AV18) interaction. The equation of state is calculated using two-body central potentials for ΛN and $\Lambda\Lambda$ interactions that are determined in order to reproduce the experimental data on single- and double- Λ hypernuclei. For the odd-state part of the $\Lambda\Lambda$ interaction, which is not known due to the lack of experimental data, a proposed repulsive and attractive potential is employed to calculate the equation of state. It is shown that the presence of Λ in the hypernuclear matter produces a strong softening of the equation of state. The results are compared with similar calculations with another variational method. The state-dependent energy as well as central and tensor correlation functions are studied up to $J = 2$ for each JLSTMT channel where related to total (J), orbital (L) and spin (S) angular momentum and isospin (T) and the third component of isospin (MT) respectively for ΛN and $\Lambda\Lambda$ interactions. Furthermore, the effect of baryon density and hyperon density as well as the type of hyperon-hyperon interaction on the two-body correlation functions are investigated.

DOI: [10.1103/PhysRevC.100.044314](https://doi.org/10.1103/PhysRevC.100.044314)

I. INTRODUCTION

The structure and properties of nuclear matter remain an open question which impacts nuclear and particle physics and astrophysics. The study of nuclear matter is important for the development of density functional theory in the study of nuclear structure, and for a deep understanding of the baryon-baryon interaction (see Ref. [1] for more details). Hyperons provide a new candidate for a strange degree of freedom in the equation of state (EoS) of nuclear matter at high densities. The presence of hyperons causes a softening of the nuclear matter EoS [2]. For calculation of the energy of nuclear matter and medium-heavy nuclei, various many-body theories [3,4] have been developed. One can mention the self-consistent Green's function scheme [5–12], the diagrammatic expansion methods, in particular the Brueckner-Bethe-Goldstone hole-line expansion [3], the Monte Carlo method in its different versions [13–18], and the variational method [19–26]. The explanation of the correlation structure of nuclear matter, which is one of its most important characteristics, is one of the main aims of this attempt through the years. In fact, the correlation function describes a correlation hole between two baryons produced by the presence of a hard core in the baryon-baryon interaction. All of the physical information about the properties and the parameters of two baryons interacting in the hypernuclear medium should be included in the correlation function. It is a key quantity to characterize a many-body technique and to realize the corresponding numerical results. The spectral function of a many-fermion system gives the important quantities of interest in scattering studies. Two important factors for calculating the spectral functions are short- and long-range correlation functions [27]. The relation between the spectral function and the correlation function is

not straightforward, but it has been studied in the Brueckner-Hartree-Fock (BHF) framework [28] and for the lowest order constrained variational (LOCV) method [29]. In the LOCV method, it is assumed that there is a specific form for the long-range behavior of the correlation functions due to an exact functional minimization of two-body energy with respect to the short-range parts of the correlation functions. However, some phenomena like dissipation due to shear viscosity and related neutrino transport [30] that occur in neutron star matter are linked to the correlation function. Therefore, it is natural to look for a calculation of the correlation functions as well as the EoS of hypernuclear matter from a reliable many-body scheme. The LOCV method was developed [31,32] for calculating the properties of homogeneous nuclear fluids in a series of works with realistic nucleon-nucleon interactions [33,34]. Furthermore, it was generalized [35] to contain more sophisticated nucleon-nucleon interactions such as the Urbana V14 (UV14), the Argonne V14 (AV14) [36,37], and the new Argonne V18 (AV18) [38] as well as the Reid68 [33] and Δ -Reid68 [34] interactions. The LOCV calculations are also applied both at zero and finite temperatures [39,40]. The results show that it can reasonably define the nucleonic-matter properties at zero and finite temperatures [31,32,35,39,41]. The LOCV method was also extended for calculating different properties of nuclear fluids such as the hot and frozen neutron as well as the nuclear and β -stable matter with realistic nucleon-nucleon interactions [35,40,41]. The nucleon-nucleon (NN) interaction in this method was also supplemented by the Urbana-type three-body force (TBF) in Ref. [42]. Recently, the chemical potential of nucleons was calculated within the LOCV method, and also the β -stable equations in the presence of free hyperons was solved [2].

The hyperonic degree of freedom has the potential for great impact on the properties of dense nuclear matter. A hyperon is a baryon containing one or more strange quarks, but no charm, bottom, or top quark. Astrophysical research has shown that this form of matter most likely exists in a stable form within the core of neutron stars [43–48]. So far, our LOCV method does not include strange particles. With respect to the above arguments, in this work we attempt to develop our method by including hyperons as a strange particle for the first time. In this choice, we pay particular attention to the Λ hyperon in the LOCV method as well as calculation of the state-dependent two-body correlation functions and the energy for each pair of particles, i.e., NN , ΛN , and $\Lambda\Lambda$. To the best of our knowledge, this is the first study for the calculation of such central and tensor correlation functions for the hyperon-nucleon and the hyperon-hyperon interactions. Of course, there are some works on the measurements of the correlation function for a pair of $\Lambda\Lambda$ or $p\Lambda$ in relativistic heavy-ion collisions [49], in which the correlation is measured as a function of the relative momentum. This kind of correlation function is sensitive to the effects of quantum statistics (QS) as well as the final state interactions (FSIs). However, we calculate the correlation function as a function of distance between two particles for every interaction channel. Since we use realistic force between the baryons, our results for the correlation function are not related to QS.

In contrast to the NN interaction which has been extensively studied, the uncertainty in the hyperon-nucleon (YN) and the hyperon-hyperon (YY) interactions is much larger due to the lack of YN scattering data and no YY scattering data. Thus, it is necessary to study the structure of hypernuclei to obtain the information on YN and YY interactions. Studying the single- and double- Λ hypernuclei, a spin-parity dependent ΛN interaction is constructed [50] so as to reproduce the experimental binding energies of light Λ hypernuclei. Furthermore, an even-state part of the $\Lambda\Lambda$ interaction is constructed [51] so as to reproduce the experimental value of the double- Λ binding energy extracted from the data of ${}^6_{\Lambda\Lambda}\text{He}$ [52]. For the odd-state part of the $\Lambda\Lambda$ interaction, which is not known due to a lack of experimental data, a proposed repulsive and attractive potential is employed for calculation of the EoS [53]. We intend to compare the obtained EoS with that of a relatively simple cluster variational method [54,55]. The structure of the article is as follows. In Sec. II we present our formalism based on the LOCV formalism and evaluation of the energy for hypernuclear matter at zero temperature. In Sec. III the baryon-baryon interactions are introduced. In Sec. IV we present our results for the energy of hypernuclear matter and the properties of the two-body correlation functions. Finally, the summary and conclusion are given in Sec. V.

II. LOCV FORMULATION

The LOCV method is one of the microscopic methods developed to calculate the bulk properties of homogeneous nuclear fluids (e.g., the saturation properties) using the realistic baryon-baryon interaction. It has been employed for various

types of nucleon-nucleon interactions such as the Reid68 and Δ -Reid [32] (the modified Reid potential with the inclusion of the isobar degrees of freedom), UV14, AV14, and AV18 [35], and the charge-dependent Reid potential (Reid93) [56]. Also, various thermodynamic properties of hot and frozen homogeneous fermionic fluids such as symmetric and asymmetric nuclear matter [57], β -stable matter [35], helium-3 [58], and electron fluid [59] have been calculated using LOCV method, with different realistic interactions. Furthermore, the LOCV formulation has been developed using a relativistically fitted potential to the nucleon-nucleon phase shifts for covering the relativistic Hamiltonian [60]. The LOCV calculation is a fully self-consistent technique with no free parameter and a state-dependent correlation function. Considering the normalization condition, as a constraint, is another advantage of the LOCV formulation. This assumption keeps the higher-order terms as small as possible. In the LOCV method, it is also assumed that there is a specific form for the long-range behavior of the correlation function to carry out an exact functional minimization of two-body energy with respect to the short-range parts of correlation functions. The functional minimization procedure causes a great computational simplification in comparison to the unconstrained methods, where the short-range behavior of the correlation functions is parametrized with the aim of going beyond the lowest order [61]. Until now, we have performed the calculations of the LOCV method for nuclear matter and helium-3 beyond the lowest order to test its convergence [62]. The energy of three-body clusters was evaluated with both the state averaged and the state-dependent correlation functions. The smallness of the normalization constraint (the convergence parameter) as well as the three-body cluster energy showed that the cluster expansion converges reasonably and, neglecting the higher-order terms (i.e., more than two-body cluster), is an appropriate approximation at least up to twice the empirical nuclear matter saturation density. We extend our method to include a strange particle, i.e., Λ , for the first time.

In the LOCV method for the single-particle states, we use an ideal Fermi gas wave function, ϕ , and we employ the variational techniques to find the wave function of the interacting system [31,32,35], i.e.,

$$\Psi(1, \dots, A) = F(1, \dots, A)\Phi(1, \dots, A), \quad (1)$$

where Φ is the uncorrelated Fermi system wave function (Slater determinant of plane waves) and $F(1, 2, \dots, A)$ is the many-body correlation function. In Jastrow form, they are defined as a product of $f(ij)$ s which are two-body correlation functions, i.e.,

$$F = S \prod_{i>j} f(ij), \quad (2)$$

where S is the symmetrizing operator and in this extended LOCV formulation i, j stand for n, p , and Λ . To the best of our knowledge, central and tensor correlation functions for YN and YY interactions, which are state dependent, have not been calculated so far. The Jastrow two-body correlation functions

$f(ij)$ are defined as

$$f(ij) = \sum_{\alpha,p=1}^3 f_{\alpha}^p(ij) O_{\alpha}^p(ij), \quad (3)$$

where O_{α}^p is the projection operator which projects onto the α channels, i.e., $\alpha = \{J, L, S, T, T_z\}$. For singlet and triplet channels with $J = L$, we choose $p = 1$ and for triplet channels with $J = L \pm 1$ we set $p = 2, 3$. The operators O_{α}^p are given by

$$O_{\alpha}^{p=1-3} = 1, \left(\frac{2}{3} + \frac{1}{6}S_{12}\right), \left(\frac{1}{3} - \frac{1}{6}S_{12}\right), \quad (4)$$

where $S_{12} = 3(\sigma_1 \cdot \hat{r})(\sigma_2 \cdot \hat{r}) - \sigma_1 \cdot \sigma_2$ is the tensor operator. The many-body energy $E[f]$ is calculated from the expectation value of our Hamiltonian, i.e.,

$$H = \sum_i \frac{p_i^2}{2m_i} + \sum_{i<j} V(ij) + \dots, \quad (5)$$

where $p_i = -\hbar\nabla_i$, m_i is the mass of the i th particle, and $v(ij)$ is the realistic two-body potential. The expectation value of energy, which is a functional of the two-body correlation function, is written in the following form using cluster expansion [63]:

$$E[f] = \frac{1}{A} \frac{\langle \Psi | H | \Psi \rangle}{\langle \Psi | \Psi \rangle} = E_1 + E_{MB} \cong E_1 + E_2 + \dots, \quad (6)$$

where A is the total number of baryons. In the lowest order we cut off the above series after E_2 . Due to the rapid convergence of the cluster expansion, the small contribution of higher-order terms is neglected in the series. The one-body energy E_1 is independent of f and is only the familiar Fermi gas kinetic energy, given by

$$E_1 = \sum_i \frac{3\hbar^2 k_{f_i}^2}{10m_i}, \quad (7)$$

where k_{f_i} is the Fermi momentum of the i th particle. Also, the two-body energy is defined as

$$E_2 = \frac{1}{2A} \sum_{ij} \langle ij | W(12) | ij - ji \rangle, \quad (8)$$

where

$$W(12) = -\frac{\hbar^2}{2m} [f(12), [\nabla_{12}^2, f(12)]] + f(12)V(12)f(12). \quad (9)$$

The two-body antisymmetrized matrix element $\langle ij | W | ij - ji \rangle$ is calculated with respect to the plane waves of single particles, i.e., ϕ . In our extended LOCV formulation which includes strange particles in addition to nucleons, the particle state, i.e., $|ij\rangle$, is defined as

$$|ij\rangle = |k_i k_j, \sigma_i \sigma_j, \tau_i \tau_j, s_i s_j\rangle. \quad (10)$$

The above quantum numbers stand for the wave number, the spin state, the isospin state, and the strange number of two particles, respectively. Therefore, we find different states for the particles with respect to the above definition, i.e.,

$|nn\rangle, |pp\rangle, |np\rangle_{T=1}$ (hereafter we denote it by $np1$), $|np\rangle_{T=0}$ (hereafter we denote it by $np0$), $|n\Lambda\rangle, |p\Lambda\rangle$, and $|\Lambda\Lambda\rangle$. A complete set of two particle states is inserted twice in the above equation. By performing some algebra, we can rewrite the two-body term as a functional of correlation functions [32,35,56]. In the above equations, $V(12)$ is a phenomenological nucleon-nucleon, nucleon-hyperon, and hyperon-hyperon potential. The expression of two-body energy can now be minimized with respect to the channel correlation function, but subject to the normalization constraint [32,35,56], which is considered in the LOCV method by

$$\chi = \frac{1}{A} \sum_{ij} \langle ij | F_p^2 - f^2 | ij - ji \rangle = 0, \quad (11)$$

where F_p is the modified Pauli function, defined by

$$F_p(r) = \begin{cases} \left[1 - \frac{9}{2} \left(\frac{J_1(k_{f_i} r)}{k_{f_i} r}\right)^2\right]^{-\frac{1}{2}}, & \text{indistinguishable particles} \\ 1, & \text{distinguishable particles,} \end{cases}$$

where $J_1(k_{f_i} r)$ denotes the spherical Bessel function of order 1. Thus, our constraint has the first form of Pauli function for $|nn\rangle, |pp\rangle$, and $|\Lambda\Lambda\rangle$, while for $|np1\rangle, |np0\rangle, |n\Lambda\rangle$, and $|p\Lambda\rangle$ we use the second form of Pauli function in the calculation of constraint. It is worth mentioning that in the cluster expansion, $[\chi = \langle \Psi | \Psi \rangle - 1]$ plays the role of a smallness parameter. All correlation functions are coupled through the Lagrange multiplier λ which is introduced to the formulation by the above constraint. Then we obtain the sets of uncoupled and coupled Euler-Lagrange differential equations with respect to the correlation functions which are related to the two-body potential. Solving these Euler-Lagrange equations, the constraint is incorporated only up to a certain distance, i.e., healing distance, where the logarithmic derivative of correlation functions matches those of the Pauli function. We can substitute thus the correlation function with the Pauli function. As mentioned before, there is no free parameter in our LOCV formulation; thus the healing distance is determined directly through the constraint and the initial conditions.

III. INTERACTIONS

As it was shown in the previous section, the expectation value of the energy will be calculated using the cluster expansion. In Eq. (9), $V(12)$ is a phenomenological two-body potential. In our method, the hypernuclear Hamiltonian is decomposed into seven parts with respect to the isospin of each pair of particles, i.e., $nn, pp, np (T = 1, 0), \Lambda p, \Lambda n$, and $\Lambda\Lambda$, where each pair will have special potential. Therefore, we obtain a two-body energy for each pair which is a functional of the two-body correlation function. As pointed out before, all of the physical information about two-baryon interactions should be included in the correlation function.

A. The nucleon-nucleon interaction

As for the NN interaction, i.e., V_{nn}, V_{pp} , and V_{np} , we employ the AV18 potential [38] which can reasonably reproduce observable data.

TABLE I. The parameters of the ΛN interaction in Eq. (12).

i	1	2	3
β_i (fm)	1.60	0.80	0.35
$v_i(1E)$ (MeV)	-7.87	-357.4	6132.0
$v_i(3E)$ (MeV)	-7.89	-217.3	3139.0
$v_i(1O)$ (MeV)	-1.30	513.7	8119.0
$v_i(3O)$ (MeV)	-3.38	22.9	5952.0

B. The Λ -nucleon interaction

In the present study, we extend the LOCV method for asymmetric nuclear matter to calculate the energies of hypernuclear matter. In particular, as for the first step, we take into account the presence of a Λ hyperon in nuclear matter. For the ΛN interaction, on the basis of the SU(3) symmetry of meson-baryon coupling constants, several meson-theoretical models have been proposed, where all of them can be used directly in our method. However, we use a spin-parity dependent potential [50] in which some parameters are tuned phenomenologically to reproduce the experimental values of the splitting energies of ${}^7_{\Lambda}\text{Li}$, simulating the basic features of the Nijmegen meson-theoretical models NSC97f [64]. We use the central part of potential which is given by [50]

$$V_{\Lambda N}^{(c)}(r) = \sum_{\alpha} \sum_{i=1}^3 v_i^{\alpha} \exp[-(r/\beta_i)^2]. \quad (12)$$

The parameters of the potential are given in Table I. In this equation, which is a three-range Gaussian form, α stands for the four different spin-parity states of the system, i.e., $\alpha = 3E$ (the triplet even), and $1E$ (the singlet even), $3O$ (the triplet odd), and $1O$ (the singlet odd). The ΛN scattering phase shifts calculated by NSC97f are simulated by the central potential. The second-range strengths of the even-state part and the odd-state part of this potential are calibrated so as to reproduce the experimental values obtained for ${}^4_{\Lambda}\text{H}$ and ${}^7_{\Lambda}\text{Li}$, respectively.

C. The $\Lambda\Lambda$ interaction

Taking into account the presence of a Λ hyperon in nuclear matter, it is necessary to consider the $\Lambda\Lambda$ potential. As in the case of ΛN interaction, we employ a central potential constructed by the same group [51] for the even-state part of the $\Lambda\Lambda$ interaction, since the experimental data obtained from hypernuclei are available for the even-state part. One should note that the experimentally known state of two Λ s in the double- Λ hypernuclei is an S orbital. As reported in Ref. [51],

 TABLE II. The parameters of the even-state part of the $\Lambda\Lambda$ interaction in Eq. (13).

i	1	2	3
μ_i (fm $^{-2}$)	0.555	1.656	8.163
v_i (MeV)	-10.67	-93.51	4884.0
v_i^{σ} (MeV)	0.0966	16.08	915.8

 TABLE III. The parameters of the odd-state part of the $\Lambda\Lambda$ interaction in Eq. (14). The parameters μ_i are chosen to be the same as the even state in fm $^{-2}$ (i.e., $\mu_1 = 0.555$, $\mu_2 = 1.656$, $\mu_3 = 8.163$).

	Attractive type	Repulsive type
v_1^{odd} (MeV)	-10.67	-1.067
v_2^{odd} (MeV)	-93.51	109.4
v_3^{odd} (MeV)	4884	4884
$v_1^{\sigma,\text{odd}}$ (MeV)	0.0966	0.00966
$v_2^{\sigma,\text{odd}}$ (MeV)	16.08	-18.81
$v_3^{\sigma,\text{odd}}$ (MeV)	915.8	915.8

the explicit form of the potential is

$$V_{12}^{\Lambda\Lambda,\text{even}} = \sum_{i=1}^3 (v_i^{\text{even}} + v_i^{\sigma,\text{even}}\sigma_1\sigma_2) \exp[-\mu_i^{\text{even}}r_{12}^2]. \quad (13)$$

One can realize that this potential is again a three-range Gaussian form, where $i = 1, 2$ are adjusted so as to simulate the $\Lambda\Lambda$ part of the NF version of the Nijmegen model. Also, the strength of the third part ($i = 3$) is returned so as to reproduce the experimental $\Lambda\Lambda$ binding energy in ${}^6_{\Lambda\Lambda}\text{He}$, which is given by a NAGARA event [the event of observation of (Lambda Lambda) He-6 double hypernucleus] [52]. The value of the parameters determined are given in Table II. As mentioned before, the odd-state part of the $\Lambda\Lambda$ interaction is not known due to the lack of experimental data. However, to calculate the EoS of the system, we employ a proposed repulsive and attractive potential model [53]. The odd-state part of the $\Lambda\Lambda$ interaction is expressed in the same form as the even-state part, but with different adjusted parameters, i.e.,

$$V_{12}^{\Lambda\Lambda,\text{odd}} = \sum_{i=1}^3 (v_i^{\text{odd}} + v_i^{\sigma,\text{odd}}\sigma_1\sigma_2) \exp[-\mu_i^{\text{odd}}r_{12}^2]. \quad (14)$$

The parameters are given in Table III.

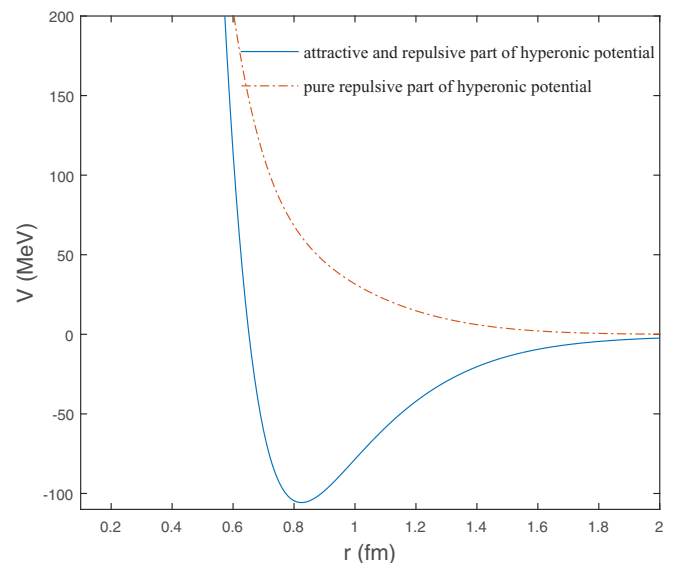


FIG. 1. The general behavior of hyperon-nucleon and hyperon-hyperon potential.

In Fig. 1 we show the general behavior of these kinds of hyperonic potential in different channels for the different states of spin and parity. All potentials expressed by Eqs. (12)–(14) have a repulsive and attractive part based on LS (orbital and spin angular momentum) channels.

IV. RESULTS AND DISCUSSION

A. The EoS of hypernuclear matter

The EoS for many-body systems is a fundamental quantity to describe the characteristics of matter and it is strongly related to the kind of particles and their interaction. In hypernuclear matter, which includes hyperons in addition to nucleons as a new degree of freedom, we expect to see a

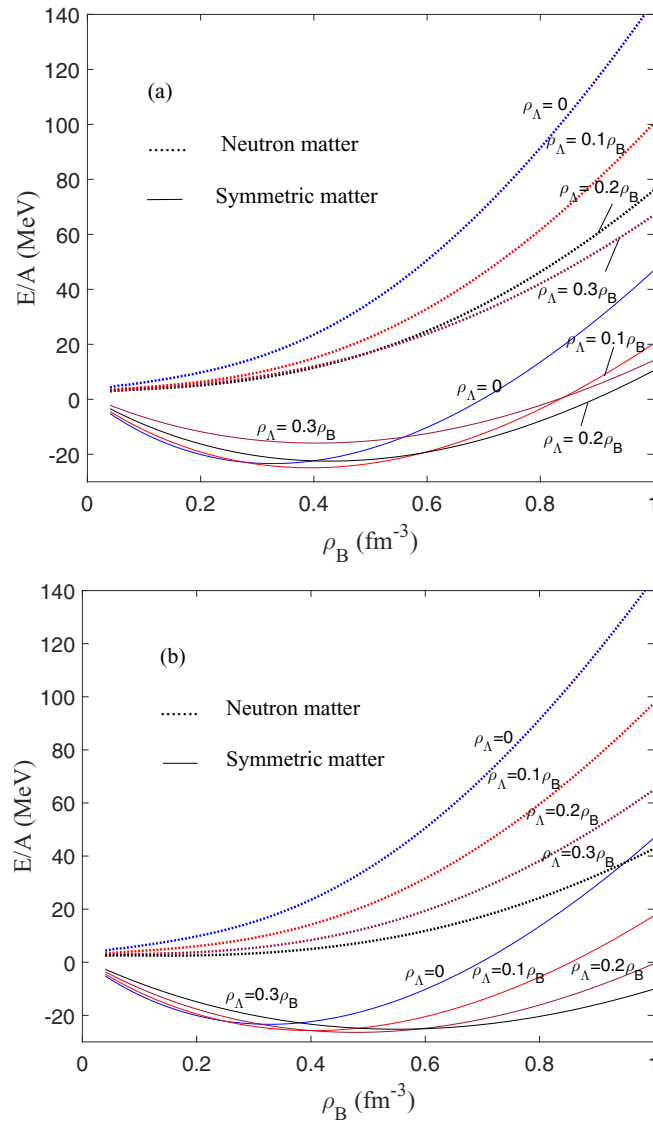


FIG. 2. The equation of state of hypernuclear matter as a function of baryon density for different x_Λ . The solid lines show the case of symmetric nuclear matter which includes Λ while the dotted lines correspond to the case of $x_p = 0$, by using (a) the repulsive odd-state part of the $\Lambda\Lambda$ interaction and (b) the attractive odd-state part of the $\Lambda\Lambda$ interaction.

softer equation of state in comparison to nuclear matter. Furthermore, one expects the hyperons to appear in the nuclear matter when the density increases and the chemical potential of nucleons can supply the rest mass of hyperons. Thus, a reliable microscopic method should include hyperons. For the first time, we supplement the LOCV method to contain an interacting hyperon and calculate the EoS of hypernuclear matter with different proton fractions (x_p) as well as different lambda fractions (x_Λ). As discussed in our previous work [2], in the presence of hyperons, there is no significant change in the EoS of hypernuclear matter with and without nucleonic TBF at densities around nuclear saturation density. Therefore, in this work we devote our calculation to the case without nucleonic TBF. However, it is worth mentioning that, without including TBF, the maximum mass of a neutron star cannot fulfill the observational lower bound on the value of the compact star maximum mass [2] and the saturation properties of the nuclear matter cannot be reproduced correctly but these calculations have not been the goal of the present study and we will consider them in a future work.

In Fig. 2, we show the energy per baryon as a function of baryon density with the repulsive [Fig. 2(a)] and attractive [Fig. 2(b)] types of odd-state $\Lambda\Lambda$ interaction, respectively. The solid lines show the energy of symmetric nuclear matter which includes a different fraction of Λ , while the dotted lines indicate the case where the proton fraction is zero. Therefore, the dotted line with the zero Λ fraction corresponds to the pure neutron matter. It is worth mentioning that our LOCV method is a flexible method for calculation of the EoS for hypernuclear matter with any arbitrary magnitude of (x_p) and (x_Λ). The role of hyperon inclusion to soften the EoS is clear in Fig. 2. As it can be observed from the figures, the behavior of the total energy (which does not include the rest mass of particles) with increasing the Λ fraction is different at low and high densities. In particular, at low densities, the contribution

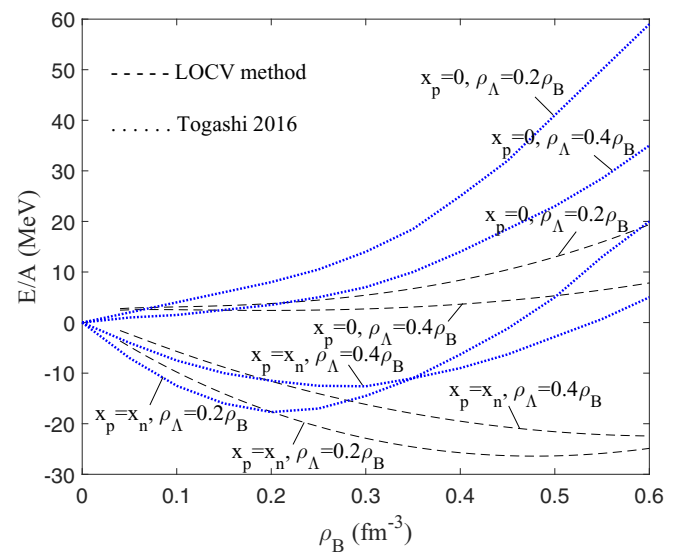


FIG. 3. The comparison of the EoS for hypernuclear matter calculated within the LOCV method and the variational method used in the work of Togashi *et al.* [53]. In both methods, the same interactions for NY and YY have been used.

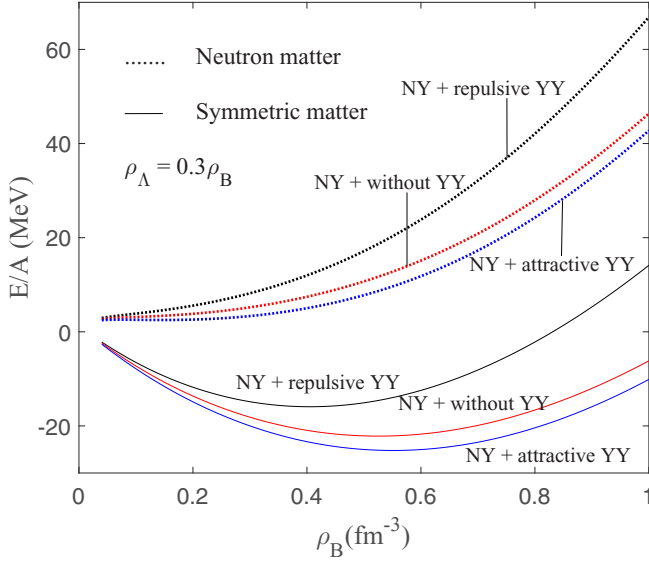


FIG. 4. The equation of state of hypernuclear matter as a function of baryon density. The cases which include an attractive $\Lambda\Lambda$ interaction and a repulsive one as well as the case in which we removed the $\Lambda\Lambda$ interaction are compared. The solid lines show the case of symmetric nuclear matter which includes Λ , while the dotted lines correspond to the case of $x_p = 0$.

of attractive nuclear force is more than that of hyperonic force; thus, the energy will increase with increasing the Λ fraction. However, at high densities, the energy decreases with increasing the Λ fraction, since more Λ hyperons with much heavier mass in comparison with nucleons occupy a single-particle state with lower energies than those of nucleons. For comparison, Fig. 3 shows the attractive type of odd-state $\Lambda\Lambda$ interaction both for the LOCV method and another variational method used in Ref. [53]. In spite of differences in calculation, the behavior of the EoS as a function of baryon density which is obtained within the LOCV method seems similar to that of Ref. [53]. The difference between magnitudes is because of the use of nucleonic TBF in Ref. [53], while we only use a two-body force between nucleons. Thus, our EoS is softer and the saturation point will appear at higher densities. In this

work, our focus is on considering a strange particle in the LOCV method and its effect on the energy per particle as well as the study of two-body correlation functions in NY and YY interactions for the first time. Thus, the effect of nucleonic TBF is not our goal in this work. However, it is studied in detail in the LOCV method [42].

For a better presentation of the effect of different kinds of $\Lambda\Lambda$ interaction, we plot Fig. 4. As can be seen in this figure, in both neutron matter and nuclear matter, including the repulsive type for odd-state $\Lambda\Lambda$ interaction causes a stiffness in the EoS in comparison with the case in which the $\Lambda\Lambda$ interaction is removed. Furthermore, as expected, considering the attractive type for odd-state $\Lambda\Lambda$ interaction results in more softening.

Since the study of the correlation function of $\Lambda\Lambda$ in heavy-ion collisions shows that $\Lambda\Lambda$ interaction is weak and mainly attractive [49], hereafter we devote our results to the attractive $\Lambda\Lambda$ interaction. It should be pointed out that, at high densities, an attractive $\Lambda\Lambda$ interaction can result in the formation of strangelets in the core of neutron stars [65,66]. In Table IV, we present the contribution of every channel in the energy of hypernuclear matter and nuclear matter for comparison up to $J = 2$ at $\rho_B = 0.3 \text{ fm}^{-3}$, and $\rho_\Lambda = 0.3\rho_B$ when $x_p = x_n$.

Note that the magnitudes listed in Table IV are the two-body energies for every channel given by Eq. (8) which are calculated within the LOCV method. Thus, for obtaining the total energy, one should add the one-body energy (i.e., kinetic energy) which is given by Eq. (7), and in this case it is equal to 24.59 MeV for hypernuclear matter and 33.61 MeV for nuclear matter, which results in a total energy of -19.99 MeV for hypernuclear matter and -23.23 MeV for nuclear matter. As stated before (also see Fig. 2), the contribution of attractive channels in the energy for nuclear matter is more than hypernuclear matter in this baryon density. Furthermore, for $J \leq 2$, there is not much difference between the energies of various isospin projection in different channels. Figure 5 shows the density dependence of 1S_0 and 3S_1 channels, which have the main contribution in the two-body energy for cases with and without Λ . As the figure shows, both calculations have the same density dependence.

We compare our results for energy with the energies of hypernuclei determined experimentally [67] or calculated so

TABLE IV. Comparison of channel breakdown of energy (MeV) for hypernuclear matter and nuclear matter up to $J = 2$ at $\rho_B = 0.3 \text{ fm}^{-3}$ and $\rho_\Lambda = 0.3\rho_B$ when $x_p = x_n$.

Channel	pp	nn	$\Lambda\Lambda$	$np1$	$np0$	$p\Lambda$	$n\Lambda$	$\sum M_T$	No Λ
1S_0	-4.46	-4.49	-0.68	-4.60				-14.23	-24.13
3P_0	-0.99	-1.00	-0.18	-0.92				-3.09	-5.29
1P_1					3.23	0.09	0.10	3.43	7.25
3P_1	2.77	2.77	-0.54	2.66				7.66	19.07
3S_1					-15.81	-4.75	-4.51	-25.07	-26.06
3D_1					0.96	-0.12	-0.12	0.72	2.55
1D_2	-0.86	-0.86	-0.07	-0.83				-2.62	-6.06
3D_2					-3.6	-0.2	-0.2	-4.00	-8.20
3P_2	-2.15	-2.16	-0.44	-2.12				-6.87	-14.76
3F_2	-0.17	-0.18	-0.01	-0.15				-0.51	-1.22
Total	-5.87	-5.92	-1.92	-5.21	-15.22	-4.98	-4.73	-44.59	-56.84

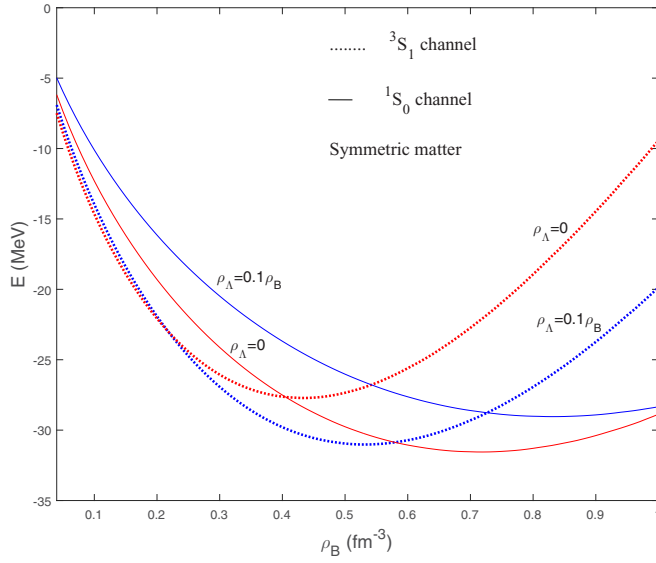


FIG. 5. The comparison of 1S_0 and 3S_1 channel contributions to the binding energy for nuclear matter and hypernuclear matter.

as to reproduce reasonably the existing data for Λ -binding energy [51]. The results are presented in Table V.

In this table, as an approximation, a numerical integration was performed over the density dependent energy obtained from the LOCV method, i.e.,

$$E_{LOCV} = \int_0^\infty E(\rho)\rho(r)dv, \quad (15)$$

where it is assumed that every nucleus is produced with a finite number of nucleons distributed with a density $\rho(r)$ described by a Woods-Saxon distribution, i.e.,

$$\rho(r) = \frac{\rho_0}{1 + \exp \frac{r-R}{a}}, \quad (16)$$

TABLE V. Comparison of the energies calculated within the LOCV method with those of hypernuclei determined experimentally [67] or calculated so as to reproduce reasonably the existing data for Λ -binding energy [51].

x_Λ	$\frac{x_p}{x_n}$	E_{LOCV} (MeV)	Hypernuclei	$E_{\text{hypernuclei}}$ (MeV)
$\frac{1}{6}$	$\frac{2}{3}$	-3.9456	$^6_\Lambda\text{He}$	-3.29 [51]
$\frac{2}{6}$	1	-2.4509	$^6_{\Lambda\Lambda}\text{He}$	-7.25 [51]
$\frac{2}{7}$	$\frac{2}{3}$	-3.0912	$^7_{\Lambda\Lambda}\text{He}$	-8.47 [51]
$\frac{1}{8}$	$\frac{3}{4}$	-5.1970	$^8_\Lambda\text{Li}$	-9.30 [51]
$\frac{2}{8}$	1	-4.0321	$^8_{\Lambda\Lambda}\text{Li}$	-12.10 [51]
$\frac{1}{9}$	1	-5.8196	$^9_\Lambda\text{Be}$	-6.64 [51]
$\frac{2}{10}$	1	-5.1477	$^{10}_{\Lambda\Lambda}\text{Be}$	-15.05 [51]
$\frac{1}{89}$	$\frac{39}{50}$	-12.4604	$^{89}_\Lambda\text{Y}$	$\simeq -23$ [67]
$\frac{1}{139}$	$\frac{57}{82}$	-13.0254	$^{139}_\Lambda\text{La}$	$\simeq -24$ [67]
$\frac{1}{208}$	$\frac{82}{126}$	-13.4775	$^{208}_\Lambda\text{Pb}$	$\simeq -26$ [67]

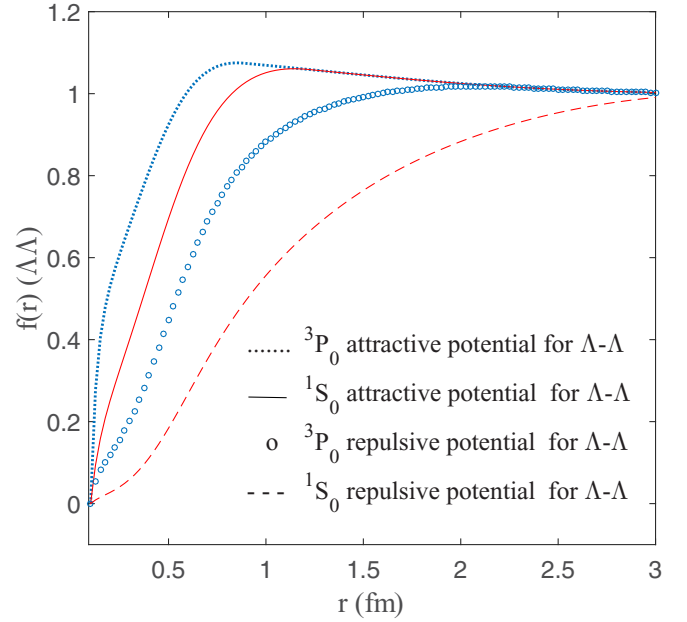


FIG. 6. The $\Lambda\Lambda$ correlation functions for both attractive and repulsive potentials in the 1S_0 and 3P_0 channels at $\rho_B = 0.17 \text{ fm}^{-3}$ and $\rho_\Lambda = 0.3\rho_B$. All the curves are plotted for the symmetric nuclear matter, i.e., $x_p = x_n$.

where ρ_0 , R , and a are the density at the center of the nucleus, the nuclear radius, and the skin depth, respectively [68]. It is worth mentioning that in our calculation the only considered term is the volume term in the mass formula and a simple central potential is used for NY and YY interactions. Nevertheless, the results of Table V show a reasonable agreement between E_{LOCV} and $E_{\text{hypernuclei}}$ in the order of magnitude for light nuclei. One should note that the effect of nucleonic TBF will be impressive; however, it lies outside the scope of this study and will be considered in a future work.

B. Correlation function

As mentioned before, the correlation functions have a key role in the study of two-baryon interactions. For the first time in this work, we present a detailed calculation on the JLSTMT channel [total (J), orbital (L) and spin (S) angular momentum and isospin (T) and the third component of isospin (MT) respectively] related to the two-body correlation functions for hyperonic two-body interaction up to $J = 2$ for every pair of the considered baryons in our method. As defined in Eqs. (3) and (4), we can calculate the central and the tensor correlation functions. As shown in Ref. [69], the results of calculated correlations look insensitive to the introduction of the TBF. Therefore, similar to the previous section, we focus our calculation on the case without TBF.

Figure 6 shows $\Lambda\Lambda$ correlation functions (CFs) for both attractive and repulsive potentials in two arbitrary interacting channels, i.e., 1S_0 and 3P_0 when ρ_B is equal to 0.17 fm^{-3} and ρ_Λ is equal to $0.3\rho_B$. This is a good test for the results of our method, because as the figure shows and we expected, the CFs in both channels clearly have shorter range for attractive

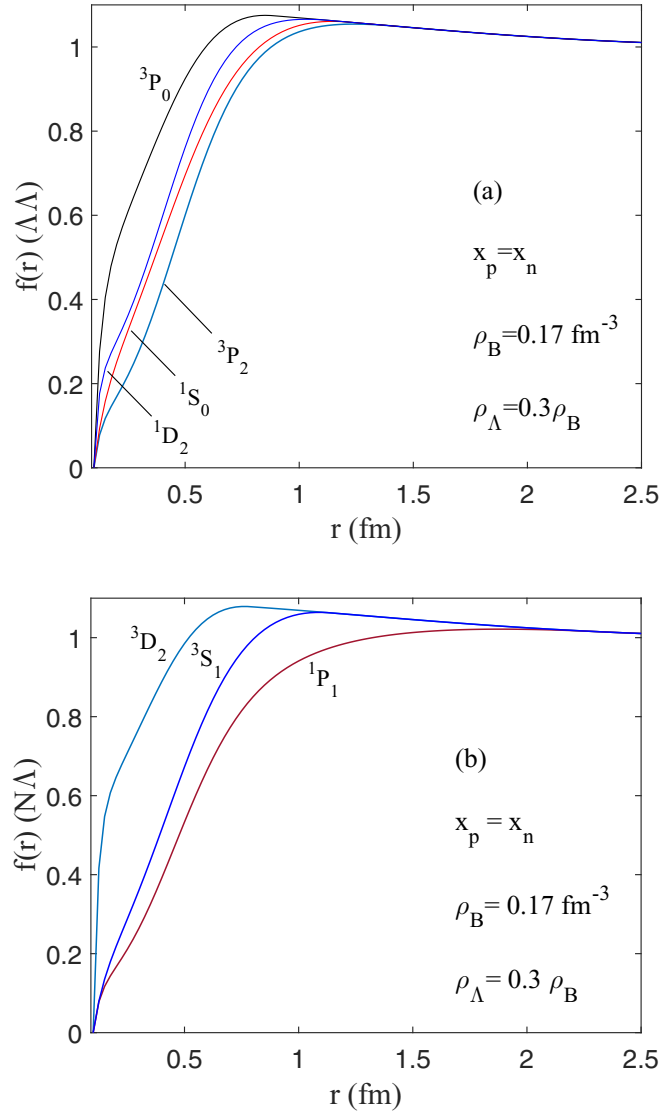


FIG. 7. The correlation functions using the attractive potential for the odd part in all interacting channels for $J \leq 2$ at $\rho_B = 0.17 \text{ fm}^{-3}$ and $\rho_\Lambda = 0.3\rho_B$, for (a) $\Lambda\Lambda$ interaction and (b) $N\Lambda$ interaction.

potential. This means that for the attractive force, the particles correlate over a shorter distance. By multiplying them in two-body plane waves, as all behavior is reflected in CFs, it means that the probability of finding two particles at shorter distances for the attractive potential is more than that for the repulsive potential.

The $\Lambda\Lambda$ CFs for $J \leq 2$ channels are plotted in Fig. 7(a), while averaged over isospin projections. As it can be seen, the behaviors of CFs in various channels are not much different from each other. They exactly reflect the structure of the $\Lambda\Lambda$ interaction and we have employed a central potential in this case. For comparison, the CFs of $N\Lambda$ interaction for different channels are plotted in Fig. 7(b). A small hard core of radius $R_c = 0.1 \text{ fm}$ is introduced in our numerical calculation for the variational method, which is shown in the figures, since the correlation functions are zero below the core radius.

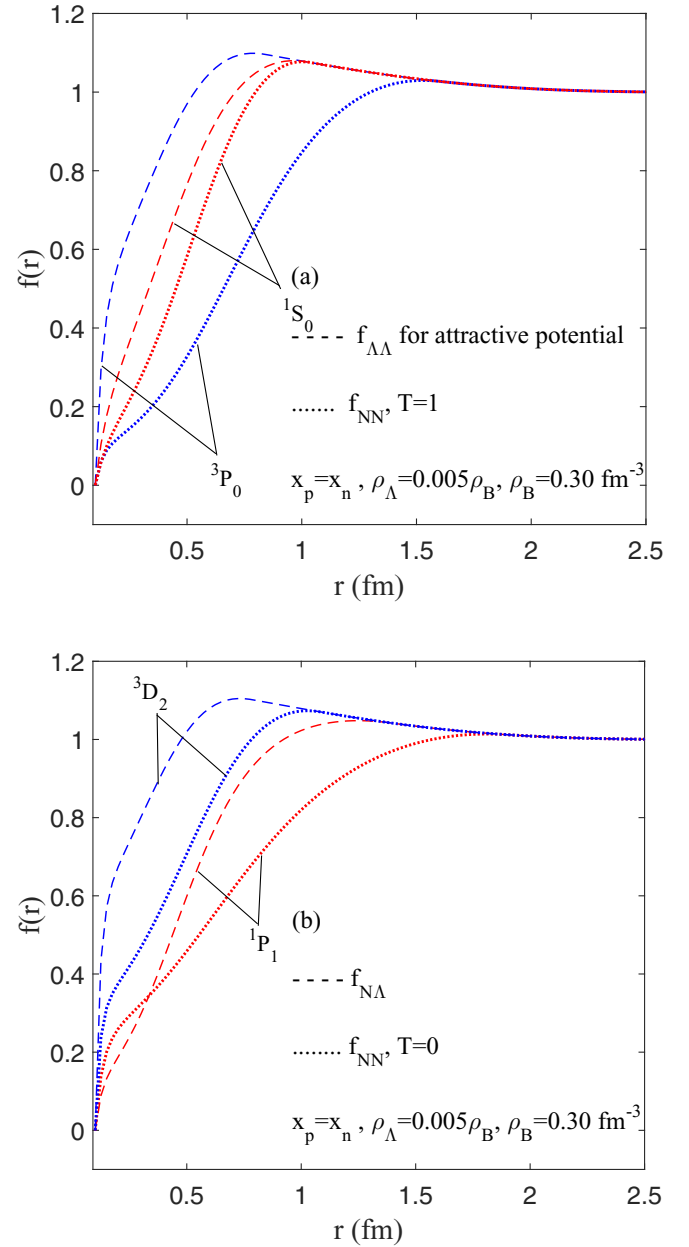


FIG. 8. The two-body correlation function at $\rho_B = 0.30 \text{ fm}^{-3}$, $\rho_\Lambda = 0.005\rho_B$, and $x_p = x_n$. (a) The correlation function of the $\Lambda\Lambda$ interaction using the attractive potential for the odd part compared with those of the NN interaction with $T = 1$. (b) The correlation function of the $N\Lambda$ interaction using the attractive potential for the odd part compared with those of the NN interaction with $T = 0$.

The CFs for hyperonic interaction are compared with those of nucleonic interaction in Fig. 8. In Fig. 8(a), we present CFs for $\Lambda\Lambda$ as well as NN with $T = 1$ for two arbitrary interacting channels. It is worth mentioning that they all interact via the same channels. In Fig. 8(b), the results of CFs for $N\Lambda$ as well as NN with $T = 0$ are compared in two arbitrary interacting channels. As it can be seen in both figures, hyperonic CFs have a shorter range. This is as expected, due to the heavier mass of hyperons which results in the shorter range for their interaction.

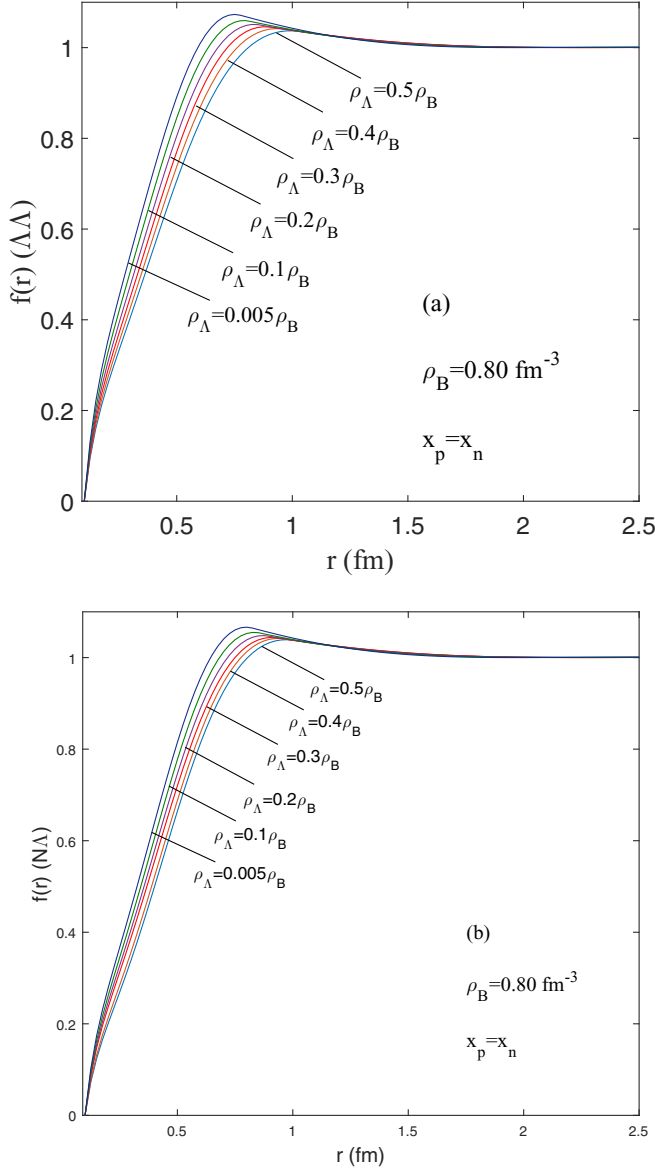


FIG. 9. The comparison of correlation functions at $\rho_B = 0.80 \text{ fm}^{-3}$ and $x_p = x_n$ for different Λ fraction: (a) $\Lambda\Lambda$ interaction for the 1S_0 channel and (b) $N\Lambda$ interaction for the 3S_1 channel.

We plotted two-body CFs for every pair of baryons in an arbitrary interacting channel for different Λ fractions. Figure 9 shows $\Lambda\Lambda$ [Fig. 9(a)] and $N\Lambda$ [Fig. 9(b)] CFs. As shown in the figures, by decreasing the Λ fraction, the range of CFs becomes shorter and in a given distance CFs have more magnitude for smaller Λ fraction. Note that the presence of hyperons not only affects the hyperonic CFs, but also changes the pure nucleonic CFs. Regarding Eqs. (3) and (4), central and tensor correlation functions for coupled channels are defined as

$$F_c = \left(\frac{2}{3}f_2 + \frac{1}{3}f_3\right), \quad (17)$$

$$F_t = \frac{1}{6}(f_2 - f_3). \quad (18)$$

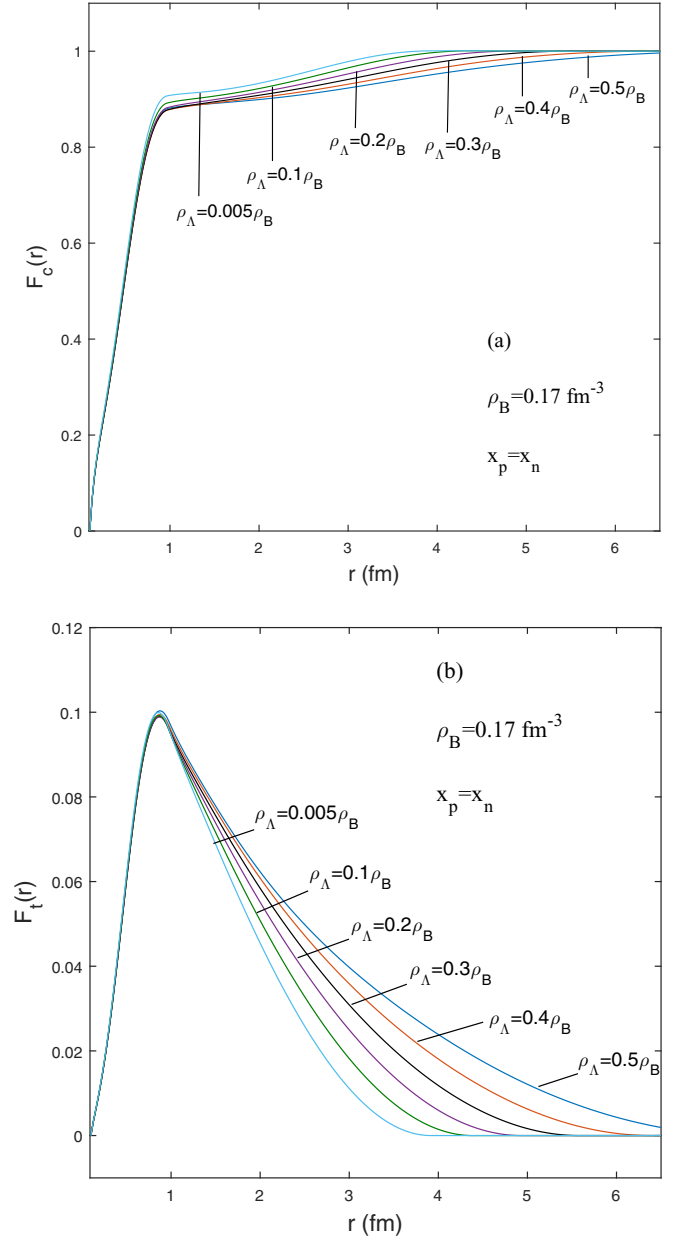


FIG. 10. The comparison of 3S_1 - 3D_1 correlation functions at $\rho_B = 0.17 \text{ fm}^{-3}$ and $x_p = x_n$ for different Λ fraction: (a) central and (b) tensor correlation function.

The central and tensor CFs can be calculated for nucleon-nucleon interaction. In Figs. 10 and 11, F_c [Figs. 10(a) and 11(a)] and F_t [Figs. 10(b) and 11(b)] are plotted for np interactions in the 3S_1 - 3D_1 coupled channel and for nn - pp interactions in the 3P_2 - 3F_2 coupled channel, respectively, in the presence of Λ . The figures show that fulfilling the LOCV constraint in the presence of a new particle changes and NN CFs show a new behavior by increasing the Λ fraction. One should notice the different scales of F_t and F_c . As it can be seen in the figures, F_t is much weaker than F_c . Furthermore, by decreasing the Λ fraction, the range of CFs becomes shorter again. This is because increasing the density of Λ affects the attractive interaction of nucleons.

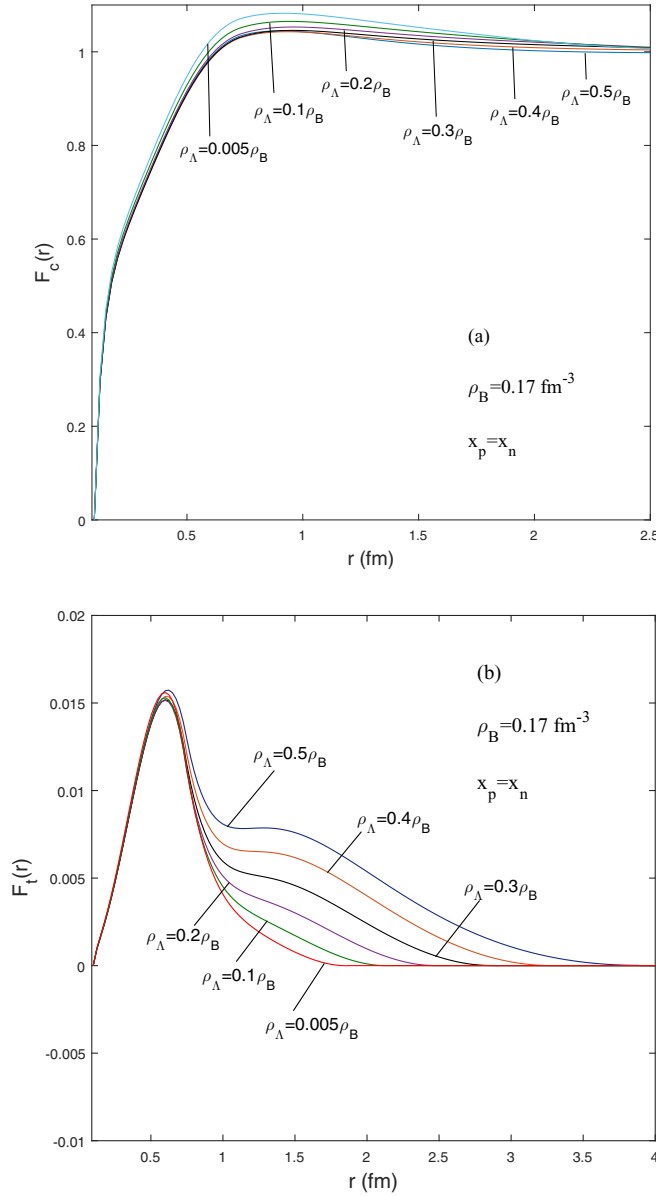


FIG. 11. The comparison of 3P_2 - 3F_2 correlation functions at $\rho_B = 0.17 \text{ fm}^{-3}$ and $x_p = x_n$ for different Λ fraction: (a) central and (b) tensor correlation function.

In addition, the effect of changing baryon density on the behavior of hyperonic CFs has been studied. We have shown that in both YY and NY interactions, by increasing ρ_B the range of CFs becomes shorter, especially over short distances. This is what we expected, because increasing the baryon density results in increasing the probability of finding two particles in a given distance. The results are shown in Fig. 12.

V. CONCLUSION

We developed the LOCV formulation for the first time to include a strange baryon, i.e., the Λ hyperon. To do so, we modified our formalism as well as the wave functions and the constraint to be employed for the new degree of freedom. We used a central potential which is spin-parity dependent

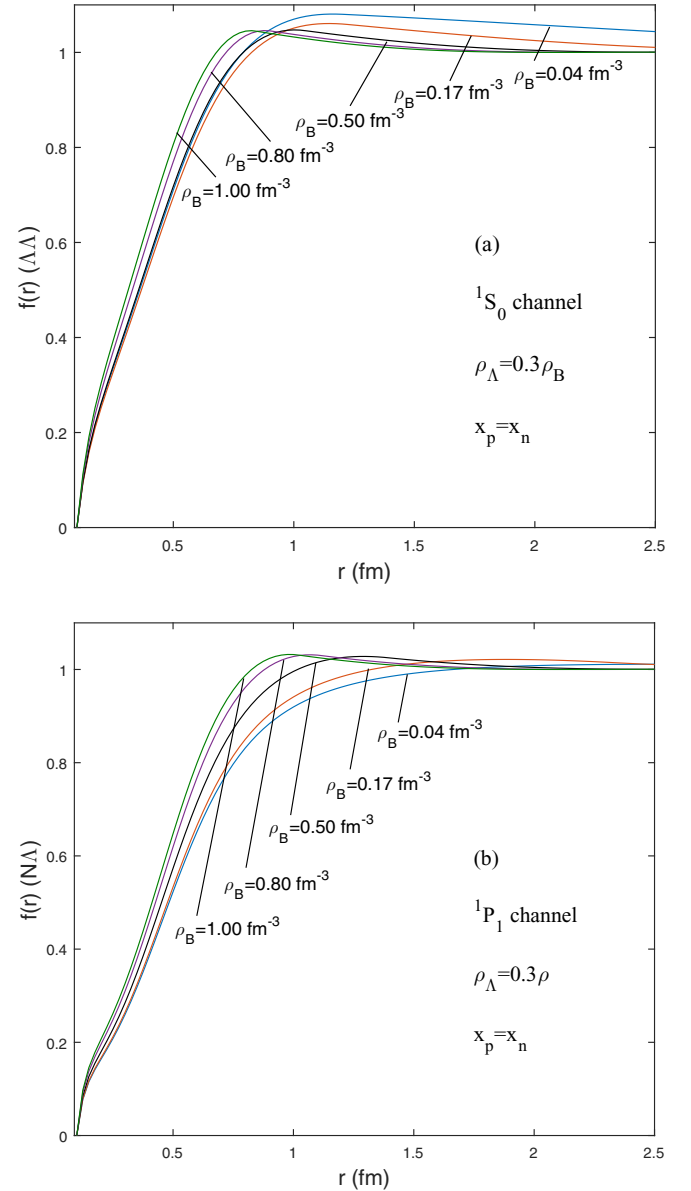


FIG. 12. The comparison of hyperonic correlation functions at $\rho_\Lambda = 0.3\rho_B$ and $x_p = x_n$ for different ρ_B : (a) $\Lambda\Lambda$ interaction for the 1S_0 channel and (b) $N\Lambda$ interaction for the 1P_1 channel.

for both nucleon-hyperon and hyperon-hyperon interactions within the LOCV method. We showed that including Λ as a new degree of freedom as well as increasing the Λ fraction causes softness in the EoS of hypernuclear matter. The behavior of the obtained EoS as a function of baryon density, neglecting the effect of nucleonic TBF, is in agreement with that of another variational calculation which employs the same potential. We have calculated the JLSTMT-channel-related two-body correlation function as a function of distance for NY and YY interactions which are performed for the first time to the best of our knowledge. The results show that hyperonic correlation functions have a shorter range in comparison with the nucleonic one. Furthermore, the effects of changing the Λ fraction as well as the baryon density were studied. It was shown that by increasing the Λ fraction, the range of the

correlation functions becomes longer as a good adaptation with observed hypernuclei with large mass number. This effect has been observed not only in the hyperonic correlation functions but also in the pure nucleonic correlation functions. It means that the probability of the presence of particles in a given distance with lower Λ fraction is more than that of the higher one. Moreover, it was shown that by increasing

baryon density, correlation functions are transferred to lower distances.

ACKNOWLEDGMENT

We would like to thank the Research Council of the University of Tehran.

-
- [1] M. Baldo and G. F. Burgio, *Rep. Prog. Phys.* **75**, 026301 (2012).
- [2] M. Shahrabaf and H. R. Moshfegh, *Ann. Phys.* **402**, 66 (2019).
- [3] M. Baldo, in *Nuclear Methods and the Nuclear Equation of State*, edited by M. Baldo (World Scientific, Singapore, 1999), Vol. 8, p. 1.
- [4] J. Navarro, R. Guardiola, and I. Moliner, in *Introduction to Modern Methods of Quantum Many-Body Theory and Their Applications*, edited by A. Fabrocini, S. Fantoni, and E. Krotscheck (World Scientific, Singapore, 2002), Vol. 7.
- [5] A. Ramos, W. H. Dickhoff, and A. Polls, *Phys. Rev. C* **43**, 2239 (1991).
- [6] T. Alm, B. L. Friman, G. Ropke, and H. Schulz, *Nucl. Phys. A* **551**, 45 (1993).
- [7] Y. Dewulf, W. H. Dickhoff, D. Van Neck, E. R. Stoddard, and M. Waroquier, *Phys. Rev. Lett.* **90**, 152501 (2003).
- [8] T. Frick and H. Muther, *Phys. Rev. C* **68**, 034310 (2003).
- [9] H. Muther and W. H. Dickhoff, *Phys. Rev. C* **72**, 054313 (2005).
- [10] I. Vidana and A. Polls, *Phys. Lett. B* **666**, 232 (2008).
- [11] A. Rios, A. Polls, A. Ramos, and H. Muther, *Phys. Rev. C* **74**, 054317 (2006).
- [12] A. Rios, A. Polls, and I. Vidana, *Phys. Rev. C* **79**, 025802 (2009).
- [13] B. S. Pudliner, V. R. Pandharipande, J. Carlson, and R. B. Wiringa, *Phys. Rev. Lett.* **74**, 4396 (1995).
- [14] K. E. Schmidt and S. Fantoni, *Phys. Lett. B* **446**, 99 (1999).
- [15] S. C. Pieper and R. B. Wiringa, *Annu. Rev. Nucl. Part. Sci.* **51**, 53 (2001).
- [16] J. Carlson, J. Morales, Jr., V. R. Pandharipande, and D. G. Ravenhall, *Phys. Rev. C* **68**, 025802 (2003).
- [17] A. Gezerlis and J. Carlson, *Phys. Rev. C* **81**, 025803 (2010).
- [18] G. Wlazlowski and P. Magierski, *Phys. Rev. C* **83**, 012801(R) (2011).
- [19] S. Fantoni and S. Rosati, *Nuovo Cimento A* **20**, 179 (1974).
- [20] V. R. Pandharipande and R. B. Wiringa, *Rev. Mod. Phys.* **51**, 821 (1979).
- [21] S. Fantoni and V. R. Pandharipande, *Phys. Rev. C* **37**, 1697 (1988).
- [22] R. B. Wiringa, V. Fiks, and A. Fabrocini, *Phys. Rev. C* **38**, 1010 (1988).
- [23] O. Benhar *et al.*, *Nucl. Phys. A* **550**, 2010 (1992).
- [24] S. Fantoni and A. Fabrocini, in *Microscopic Quantum Many-Body Theories and Their Applications*, edited by J. Navarro and A. Polls, Lecture Notes in Physics Vol. 510 (Springer, Berlin, 1998), pp. 119–186.
- [25] A. Akmal, V. R. Pandharipande, and D. G. Ravenhall, *Phys. Rev. C* **58**, 1804 (1998).
- [26] F. Arias de Saavedra, C. Bisconti, G. Co, and A. Fabrocini, *Phys. Rep.* **450**, 1 (2007).
- [27] O. Benhar and A. Fabrocini, *Phys. Rev. C* **62**, 034304 (2000).
- [28] M. Baldo, M. Borromeo and C. Ciofi degli Atti, *Nucl. Phys. A* **604**, 429 (1996).
- [29] M. Modarres and Y. Younesizadeh, *Phys. Rev. C* **85**, 054305 (2012).
- [30] M. Modarres and M. Rahmat, *Nucl. Phys. A* **921**, 19 (2014); *Physica A* **466**, 396 (2017).
- [31] J. C. Owen, R. F. Bishop, and J. M. Irvine, *Nucl. Phys. A* **277**, 45 (1976); *Ann. Phys.* **102**, 170 (1976).
- [32] M. Modarres and J. M. Irvine, *J. Phys. G* **5**, 511 (1979).
- [33] R. V. Reid, *Ann. Phys.* **50**, 411 (1969); B. D. Day, *Phys. Rev. C* **24**, 1203 (1981).
- [34] A. M. Green and P. Haapakoski, *Nucl. Phys. A* **221**, 429 (1974); A. M. Green, J. A. Niskanen, and M. E. Sainio, *J. Phys. G* **4**, 1085 (1978).
- [35] G. H. Bordbar and M. Modarres, *J. Phys. G* **23**, 1631 (1997); *Phys. Rev. C* **57**, 714 (1998); M. Modarres and G. H. Bordbar, *ibid.* **58**, 2781 (1998); M. Modarres and H. R. Moshfegh, *ibid.* **62**, 044308 (2000).
- [36] R. B. Wiringa, R. A. Smith, and T. L. Ainsworth, *Phys. Rev. C* **29**, 1207 (1984).
- [37] I. E. Lagaris and V. R. Pandharipande, *Nucl. Phys. A* **359**, 349 (1981).
- [38] R. B. Wiringa, V. G. J. Stoks, and R. Schiavilla, *Phys. Rev. C* **51**, 38 (1995).
- [39] M. Modarres and J. M. Irvine, *J. Phys. G* **5**, 7 (1979).
- [40] H. R. Moshfegh and M. Modarres, *J. Phys. G* **24**, 821 (1998).
- [41] M. Modarres, *J. Phys. G* **19**, 1349 (1993); **21**, 351 (1995).
- [42] S. Goudarzi and H. R. Moshfegh, *Phys. Rev. C* **91**, 054320 (2015).
- [43] M. Fortin, S. S. Avancini, C. Providencia, and I. Vidana, *Phys. Rev. C* **95**, 065803 (2017); M. Fortin, C. Providencia, A. R. Raduta, F. Gulminelli, J. L. Zdunik, P. Haensel, and M. Bejger, *ibid.* **94**, 035804 (2016).
- [44] F. Gulminelli, A. R. Raduta, and M. Oertel, *Phys. Rev. C* **86**, 025805 (2012); F. Gulminelli, A. R. Raduta, J. Margueron, P. Papakonstantinou, and M. Oertel, *J. Phys. Conf. Ser.* **420**, 012079 (2013).
- [45] M. Oertel and C. Providencia, *AIP Conf. Proc.* **1974**, 020007 (2018).
- [46] M. Baldo, G. F. Burgio, and H. J. Schulze, *Phys. Rev. C* **61**, 055801 (2000); **58**, 3688 (1998).
- [47] I. Vidana, A. Polls, A. Ramos, L. Engvik, and M. Hjorth-Jensen, *Phys. Rev. C* **62**, 035801 (2000).
- [48] H. J. Schulze, A. Polls, A. Ramos, and I. Vidana, *Phys. Rev. C* **73**, 058801 (2006).
- [49] L. Adamczyk *et al.* (STAR Collaboration), *Phys. Rev. Lett.* **114**, 022301 (2015).
- [50] E. Hiyama, Y. Yamamoto, T. A. Rijken, and T. Motoba, *Phys. Rev. C* **74**, 054312 (2006).

- [51] E. Hiyama, M. Kamimura, T. Motoba, T. Yamada, and Y. Yamamoto, *Phys. Rev. C* **66**, 024007 (2002).
- [52] H. Takahashi *et al.*, *Phys. Rev. Lett.* **87**, 212502 (2001).
- [53] H. Togashi, E. Hiyama, Y. Yamamoto, and M. Takano, *Phys. Rev. C* **93**, 035808 (2016).
- [54] H. Togashi and M. Takano, *Nucl. Phys. A* **902**, 53 (2013).
- [55] H. Togashi, M. Takano, K. Sumiyoshi, and K. Nakazato, *Prog. Theor. Exp. Phys.* **2014**, 023D05 (2014).
- [56] M. Modarres and H. R. Moshfegh, *Prog. Theor. Phys.* **112**, 21 (2004); H. R. Moshfegh and M. Modarres, *Nucl. Phys. A* **759**, 79 (2005).
- [57] H. R. Moshfegh and M. Modarres, *Nucl. Phys. A* **792**, 201 (2007).
- [58] M. Modarres and H. R. Moshfegh, *Physica A* **388**, 3297 (2009).
- [59] M. Modarres, H. R. Moshfegh, and A. Sepahvand, *Eur. Phys. J. B* **31**, 159 (2003).
- [60] H. R. Moshfegh and S. Zaryouni, *Eur. Phys. J. A* **43**, 283 (2010); **45**, 69 (2010).
- [61] B. Friedman and V. R. Pandharipande, *Nucl. Phys. A* **361**, 502 (1981).
- [62] M. Modarres, A. Rajabi, and H. R. Moshfegh, *Phys. Rev. C* **76**, 064311 (2007).
- [63] J. W. Clark, *Prog. Part. Nucl. Phys.* **2**, 89 (1979).
- [64] T. A. Rijken, V. G. J. Stoks, and Y. Yamamoto, *Phys. Rev. C* **59**, 21 (1999).
- [65] R. Tamagaki, *Prog. Theor. Phys.* **85**, 321 (1991).
- [66] C. Alcock, E. Farhi, and A. Olinto, *Astrophys. J.* **310**, 261 (1986).
- [67] O. Hashimoto, and H. Tamura, *Prog. Part. Nucl. Phys.* **57**, 564 (2006).
- [68] H. De Vries, C. W. De Jager, and C. De Vries, *At. Data Nucl. Data Tables* **36**, 495 (1987).
- [69] M. Baldo and H. R. Moshfegh, *Phys. Rev. C* **86**, 024306 (2012).